AIAA JOURNAL
Vol. 43, No. 12, December 2005

Measurement of Unsteady Fluid Dynamic Forces for a Mechanical Dragonfly Model

Manabu Yamamoto*
Toyota Motor Corporation, Toyota 471-8587, Japan
and
Koji Isogai†
Nippon Bunri University, Oita 870-0397, Japan

An experimental study of the aerodynamics of a dragonfly in hovering flight is conducted. Measurements are made on a mechanical flapping wing apparatus that simulates, in water, the Reynolds number and reduced frequency of the tandem wing configuration on a dragonfly. The length scale of the flapping wing model is four times larger than on a real dragonfly. The phase difference between the flapping motions of the fore- and hindwings is independently varied in the range 0–90 deg to examine the flow interaction between the wings when the dragonfly is in hovering flight. The time histories and time average values of the fluid dynamic forces and the rate of work show that, in hovering flight, there is only a small interaction between the flows over the fore- and hindwings. The experimental data are also compared with the predictions of a three-dimensional Navier–Stokes code; these comparisons show good agreement and, thus, also verify the fidelity of the experimental data.

Nomenclature

b_f	=	semichord at 75% semispan station of forewing
k	=	reduced frequency, $b_f\omega/V_f$
L_X	=	fluid dynamic force in negative X direction
L_Y	=	fluid dynamic force in Y direction
L_{hover}	=	vector sum of L_X and L_Y
P	=	rate of work
R	=	semispan of forewing
Re	=	Reynolds number, $b_f V_f/\nu$
t	=	time
V_f	=	maximum flapping velocity at 75% semispan of forewing
X, Y, Z	=	Cartesian coordinates, Y axis along stroke plane
α	=	feathering angle
θ	=	flapping angle
ν	=	kinematical viscosity
ρ	=	fluid density
ϕ_B	=	angle between body axis and horizontal
ϕ_f, ϕ_h	=	phase advance angle of feathering motion ahead of flapping motion
ϕ_s	=	stroke-plane angle
Ψ	=	phase angle between flapping motions of fore- and hindwings
ω	=	circular frequency of oscillation

Subscripts

f	=	forewing
h	=	hindwing
t	=	sum of rate of work for fore- and hindwings
0	=	amplitude of feathering and flapping motions

Superscript

$\bar{}$	=	time averaged (during one cycle) value

I. Introduction

AS is well known, many insects including dragonflies have unique flying capabilities, namely, the abilities to hover and to turn abruptly, in addition to the usual cruising flight. Among these flight modes, hovering flight is of particular interest because, except for humming birds, only insects are capable of sustained hovering flight. To clarify the mechanism underlying this capability, many experimental[1–13] and theoretical studies[14–23] have been conducted. Ellington et al.[8] and Dickinson et al.[10] proposed that the mechanisms of lift enhancement, which are more complex than in steady aerodynamics, include the phenomena of delayed stall,[8,10] vortex lift,[8,10] wake capture,[10] and rotational circulation.[10] Among these mechanisms, the latter two phenomena, wake capture and rotational circulation, have not been widely studied. Our knowledge of the other phenomena is somewhat limited. For example, Traub[22] has demonstrated in a theoretical analysis using the actuator disk theory that the vortex lift is the major contributor; it constitutes 27–50% of the lift in attached flow and approximately 23–24% of the total lift in hovering flight. Nevertheless, it is clear that further theoretical and experimental studies of the lift-generation mechanism are necessary.

In this paper, we focus attention on a dragonfly that has two pairs of wings, the fore- and hindwings, because it has a superior hovering capability compared to other insects, namely, it can hover while maintaining its body axis horizontal. The tandem wing configuration provides an additional degree of complexity to the lift-generation mechanism due to the possible flow interaction between the fore- and hindwings. As a theoretical tool to investigate the mechanism, the recent development of the three-dimensional Navier–Stokes (NS) code might be useful because it can provides not only the behaviors of the unsteady forces but also the instantaneous flow pattern, especially, the vortex flows. Isogai et al.[23] have recently presented the three-dimensional NS simulations for a typical dragonfly, *Anax parthenope julius*. They described in detail the characteristics of the unsteady aerodynamic forces, the rate of work, and the corresponding flow patterns around the wings that are experienced during its hovering flight. They also showed that the time-averaged lift and rate of work predictions from the three-dimensional NS code are in good agreement with those observed for real dragonflies[5] and with the time-averaged lift and stroke plane angle measured on a dragonfly

Received 2 February 2005; revision received 14 July 2005; accepted for publication 17 July 2005.

*Engineer, Die Design Department, Stamping Engineering Division.
†Professor, Department of Aeronautics and Astronautics; isogai@nbu.ac.jp. Associate Fellow AIAA.

robot.[12] It is clear that further experimental data, in particular time histories of the lift and rate of work, are required because these are essential not only for understanding the aerodynamic mechanism of hovering flight but also for designing insectlike microaerial vehicles. Although experimental data of the time histories of the lift acting on a single two-dimensional flapping airfoil in hover mode are available,[7,11,13] no such data are available for a flapping three-dimensional tandem wing configuration.

In the present study, we have developed a mechanical flapping wing apparatus that acts as a tandem three-dimensional wing configuration. The planforms and motions of the fore- and hindwings approximately simulate those of *Anax parthenope julius*. The model is tested in water; thus, the scale of the wings is four times larger than that of a real dragonfly and the similarity parameters, namely, the Reynolds number and the reduced frequency, are approximately matched to those of a real dragonfly. Measurements of the time histories of the lift and rate of work are made, taking into account the phase difference between the flapping motions of the fore- and hindwings. The experimental data thus obtained are compared to the three-dimensional NS simulations.[23] In the following sections, the experimental method and the results, including the comparison with the NS simulations, are presented.

II. Experimental Method

The definitions of the coordinates, forces and wing motions are shown in Figs. 1a–1c. The Y axis is taken to be the direction of the stroke plane, and the X axis is perpendicular to the Y axis. The Z axis is taken in the spanwise direction. (Therefore, a left-handed Cartesian coordinate system is used.) The fore- and hindwings are assumed to oscillate in a coupled flapping and feathering mode, in which the feathering oscillation advances 90 deg ahead of the flapping oscillation. The flapping mode is a rotational motion around the X axis as shown in Fig. 1b, where the definitions of flapping angles are also given. The feathering mode is a twisting motion (or pitching motion) around a feathering axis, as shown in Fig. 1c, where the definitions of feathering angles are also given. There is a phase difference between the flapping oscillations of the fore- and hindwings.

The wing motions applied in the present experiment can be expressed as follows.

Forewing:

$$\theta_f = \theta_{0,f} \sin \omega t \tag{1}$$

$$\alpha_f = \alpha_{0,f} \sin(\omega t + \phi_f) \tag{2}$$

Hindwing:

$$\theta_h = \theta_{0,h} \sin(\omega t + \Psi) \tag{3}$$

$$\alpha_h = \alpha_{0,h} \sin(\omega t + \phi_h + \Psi) \tag{4}$$

For the aerodynamic forces acting on the dragonfly in the hovering flight condition, we define $\overline{L_Y}$ to be the mean aerodynamic force (time-averaged value of L_Y over a cycle of oscillation) acting in the direction of the Y axis and $\overline{L_X}$ to be the time-averaged aerodynamic force in the negative direction along the X axis (Fig. 1a). The lifting force $\overline{L_{\text{hover}}}$, which is to be equal to the body weight, is then given by

$$\overline{L_{\text{hover}}} = \sqrt{\overline{L_X}^2 + \overline{L_Y}^2} \tag{5}$$

The stroke plane angle ϕ_s (Fig. 1) can be given by

$$\phi_s = \tan^{-1}\left(\overline{L_Y}/\overline{L_X}\right) \tag{6}$$

In the present study, we use *Anax parthenope julius* as a typical dragonfly. According to the observations of Azuma and Watanabe,[5] the full span length of the forewing is approximately 0.10 m and the aspect ratio is 10. The planforms of the fore- and hindwings are shown in Fig. 2.

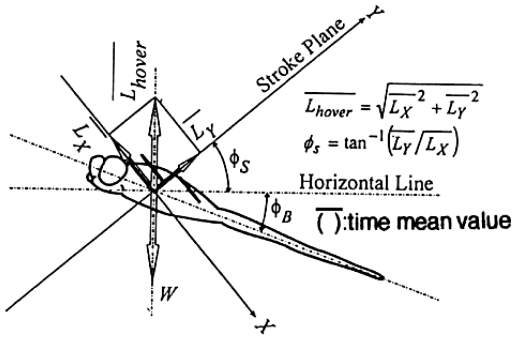

a) Forces and coordinates

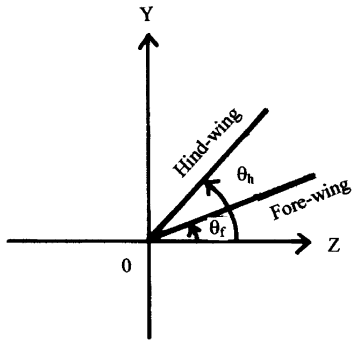

b) Flapping angles (back view)

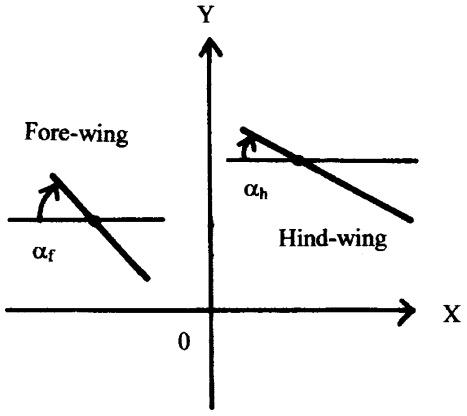

c) Feathering angles of typical spanwise station (side view)

Fig. 1 Definitions.

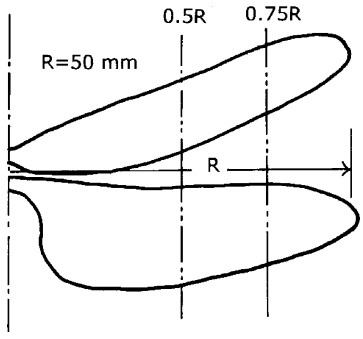

Fig. 2 Planforms of fore- and hindwings of *Anax parthenope julius*.

The semichord length at the 75% semispan station of the forewing is 0.005 m, which is taken as the reference length b_f. The flapping amplitudes of the fore- and hindwings are both 40 deg (Ref. 5). The feathering amplitudes vary linearly from the root stations to the tip stations, and they take different values depending on whether the wing motion is upward or downward. The feathering amplitude at the 75% semispan station of the forewing is 64 deg in upward motion and 40 deg in downward motion, and for the hindwing it is 51 deg in upward motion and 24 deg in downward motion.[5] The frequency

of oscillation is 28 Hz, and the maximum flapping velocity at the 75% semispan station V_f, which is taken as the reference velocity, is 4.24 m/s. The similarity parameters that govern the unsteady viscous flow for the present flapping wing problem are the Reynolds number Re and the reduced frequency k, defined as

$$Re = (b_f V_f)/\nu \tag{7}$$

$$k = (b_f \omega)/V_f \tag{8}$$

For the present dragonfly model, these parameters are $Re = 1.45 \times 10^3$ and $k = 0.207$. The body mass is 0.79×10^{-3} kg.

As already mentioned, we have designed a mechanical flapping wing apparatus that acts as a tandem wing configuration in water and whose planforms are four times larger than those of the *Anax parthenope julius*.

The flapping and feathering motions are induced by electric sliders and stepping motors, respectively. As shown in Fig. 3, these devices are controlled simultaneously by a personal computer, which sends signals to the drivers through controllers. Further details of the mechanism are shown in Fig. 4. The linear motion of the electric slider is converted into the flapping motion through a guide. An attachment to the guide, which comprises the stepping motor and the wing, rotates the shaft to generate the flapping motion of the

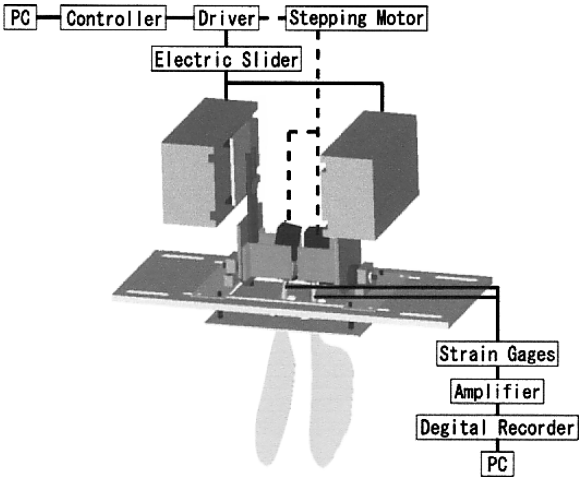

Fig. 3 Mechanical flapping wing apparatus.

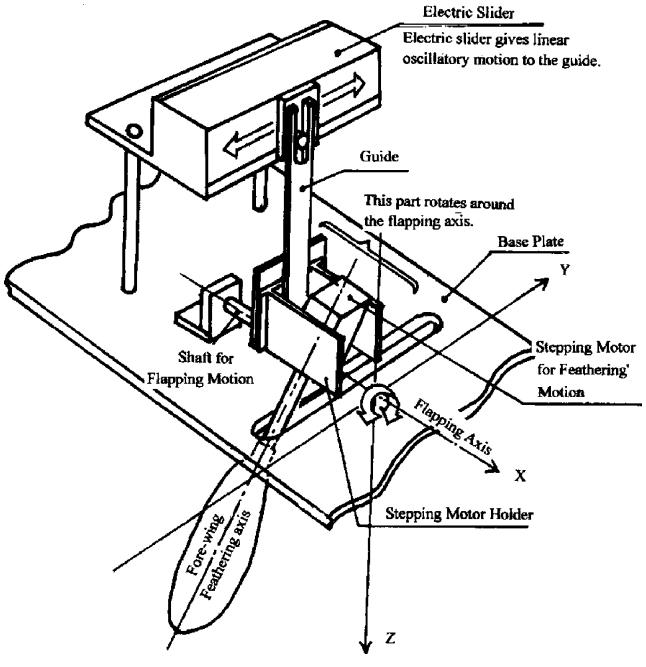

Fig. 4 Details of flapping wing mechanism.

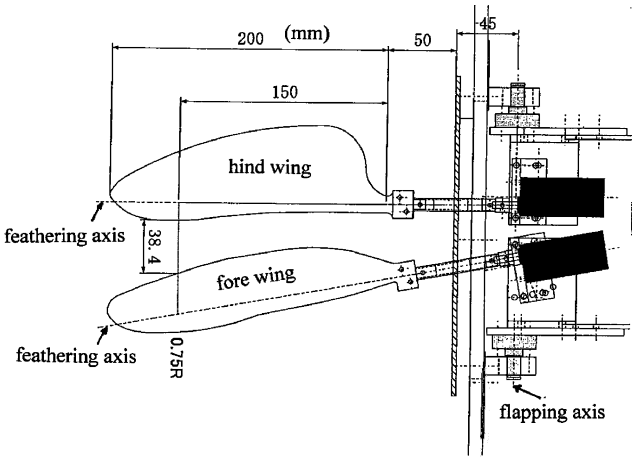

Fig. 5 Planforms and arrangement of flapping tandem wing configuration.

wing. In Fig. 5, the details of the planforms and the arrangement of the experimental wings are shown. The planforms of the wings of the apparatus are almost identical to those of real wings, though their arrangement has some differences from the dragonfly wings, due to various mechanical constraints. The primary difference is that the flapping axis of the present mechanical model is located at 95 mm (48% of the semispan length of the wings) inside from the root station of the wings, as shown in Fig. 5, whereas that of the real dragonfly is almost at the root stations of the wings. The location of the feathering axis is also shown in Fig. 5. A thin flat plate ($230 \times 190 \times 3.55$ mm) that simulates the body surface of the dragonfly is attached to the base plate that supports the electric sliders and stepping motors (Figs. 3 and 5). This thin plate prevents the movement of the free water surface as water is filled to just above the plate. The water tank has the dimension of 1.0 m high $\times$ 1.8 m wide $\times$ 0.5 m deep; thus, the effects of the proximity of the tank's bottom and sides are minimized. The distance from the tips of the wings to the bottom of the tank is more than one span length of the wings. The wings are flat plates made of stainless steel and have sufficient thickness (1.2 mm) to avoid fluid–elastic deformation. (The tip deflection induced by the maximum fluid dynamic force is estimated to be less than 6 mm, whereas the maximum movement of the tip due to the flapping motion is 190 mm. Therefore, the fluid–elastic deflection of the wing tip is less than 3% of the stroke amplitude of the tip.) The amplitudes of the flapping oscillations of the fore- and hindwings are both 40 deg. The feathering amplitudes of the wings are kept constant along the span, and their values are taken to be equal those at the 75% semispan station of the *Anax parthenope julius* dragonfly. The phase advance angle of the feathering motion ahead of the flapping motion of each wing is fixed at 90 deg, whereas the phase advance angle of the flapping motion of the hindwing ahead of the forewing is independently varied from 0 to 90 deg in 10-deg intervals. All experiments are conducted at a frequency of 0.35 Hz. Therefore, as defined by Eqs. (7) and (8), $Re = 5.62 \times 10^3$ and $k = 0.135$. The fluid dynamic forces acting on each wing are measured as follows. First, the forces acting in the direction normal to the wing surface and the torque around the flapping axis are measured using strain gauges that are attached to the shaft connecting the wing and the stepping motor. In this experiment, the forces tangential to the wings are not measured because they are estimated to be, at most, less than 1.3% of the normal forces. These tangential forces are estimated using the boundary-layer theory, in which attached laminar flow is assumed.

The details of the technique to obtain the forces and torque can be described with the aid of Fig. 6. The normal forces are calculated from the bending moments measured by using strain gauges 1 and 2, that is,

$$L_n = \int_a^b f(x)\,\mathrm{d}s = \frac{(M_1 - M_2)}{s} \tag{9}$$

where the bending moments M_1 and M_2 are measured by strain gauges 1 and 2, respectively, and they are given by

$$M_1 = \int_a^b xf(x)\,\mathrm{d}x \tag{10}$$

$$M_2 = \int_a^b (x-s)f(x)\,\mathrm{d}x \tag{11}$$

The respective distances, measured from the flapping axis, of strain gauges 1 and 2 are 30 and 70 mm, and the values of s, a, and b are 40, 65, and 265 mm, respectively. The diameter of the shaft is 9 mm. It is clear that the torque $Q(t)$ around the flapping axis can be measured using strain gauge 1 only. The rate of work is calculated as

$$P(t) = Q(t)\left(\frac{\mathrm{d}\theta}{\mathrm{d}t}\right) \tag{12}$$

L_X and L_Y are calculated from the normal force data L_n as

$$L_X = -L_n \sin\alpha \tag{13}$$

$$L_Y = L_n \cos\alpha \cos\theta \tag{14}$$

The basis of Eqs. (13) and (14) is shown in Fig. 7, where the $XY'Z'$ coordinate system is generated by rotating the XYZ system around the X axis (flapping axis) and the $X''Y''Z'$ coordinate system is generated by rotating the $XY'Z'$ system around the Z' axis (feathering axis). (Note that the XYZ, $XY'Z'$, and $X''Y''Z'$ coordinate systems are all left-handed Cartesian coordinate systems and the $X''Y''Z'$ system is fixed relative to the wing.) Because the earlier measured L_X, L_Y, and P include both the fluid dynamic forces and the inertial forces, the inertial forces are measured independently by oscillating the wings under the same conditions but in the absence of the water. These inertial contributions are then subtracted from the measurements made on the model in water to yield the fluid dynamic forces.

The signal for the flapping motion of the hindwing (which is generated from the controller of the electric slider) is used as the reference signal for all of the data processing including the corrections for the inertial forces. An analysis of the video images of the moving wings confirmed that the actual wing motions (both flapping and feathering motions) are accurately simulated without a measurable delay due to the control signals from the controllers. (The errors in the flapping and feathering angles are less than 1 deg.)

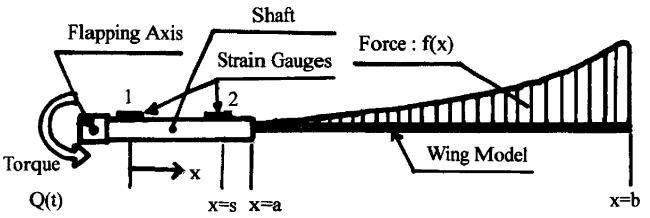

Fig. 6 Method to measure normal force and torque.

III. Results

Typical examples of the time histories of the forces and rate of work over a cycle of oscillation with a phase angle $\Psi = 40$ deg are shown in Figs. 8 and 9 for the fore- and hindwings, respectively. (Note that the values of L_X, L_Y, and P are for the full span wing.) In Figs. 8 and 9, the values computed by the three-dimensional NS code developed by Isogai et al.[23] are also plotted for comparison. The three-dimensional NS simulations are conducted for the same

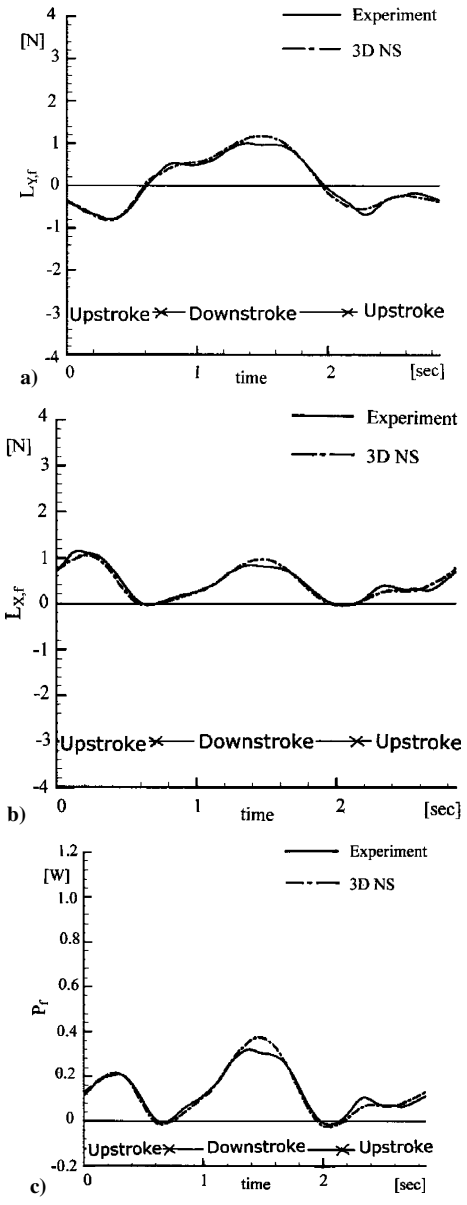

Fig. 8 $L_{Y,f}$, $L_{X,f}$, and P_f during one cycle of oscillation for $\Psi = 40$ deg for the forewing.

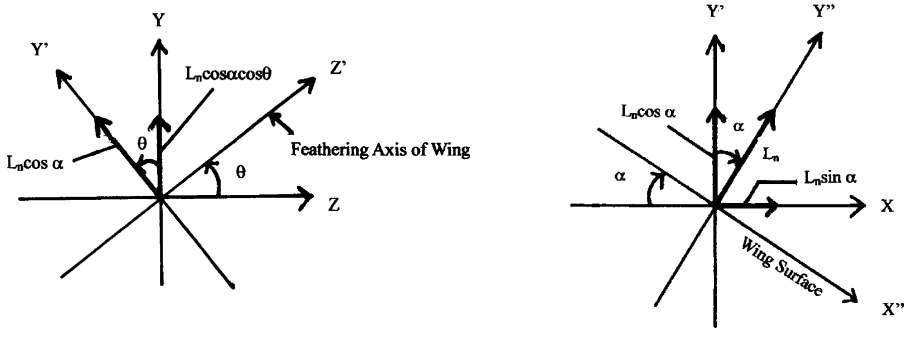

Fig. 7 Relations between L_X, L_Y, and L_n.

Table 1 Time-averaged forces and rate of work

Wing	$\overline{L_X}$, N	$\overline{L_Y}$, N	$\overline{L_{\text{hover}}}$, N	ϕ_s, deg	$\overline{P}$, W
		Experiment			
Forewing	0.488	0.122			0.140
Hindwing	0.558	0.143	1.080	14.2	0.245
Total	1.046	0.265			0.385
		Three-dimensional NS simulation			
Forewing	0.434	0.104			0.130
Hindwing	0.572	0.194	1.050	16.5	0.246
Total	1.006	0.298			0.376

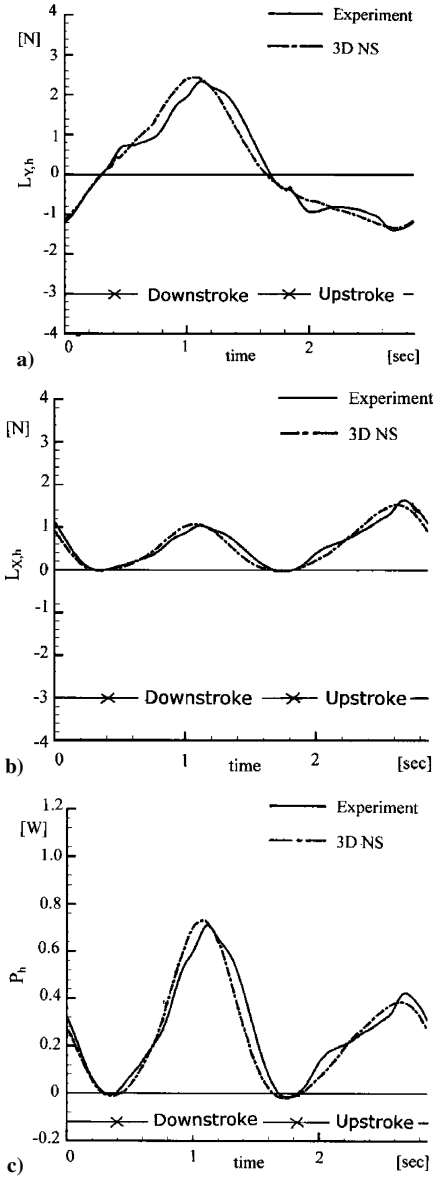

Fig. 9 $L_{Y,h}$, $L_{X,h}$, and P_h during one cycle of oscillation for $\Psi = 40$ deg for the hindwing.

configuration and wing motions as in the present experiment. On the forewing, there is a small mismatch between the experiment and NS simulations at the peaks of the time histories. However, overall the agreement is quite good. On the hindwings, there is a small phase difference between the experiment and NS simulations, but the overall magnitudes are in good agreement. Similarly, good agreement is obtained for other values of Ψ. The time-averaged values of L_X, L_Y, and P, with phase angle $\Psi = 40$ deg, are summarized in Table 1. The agreement between experiment and NS simulations is excellent.

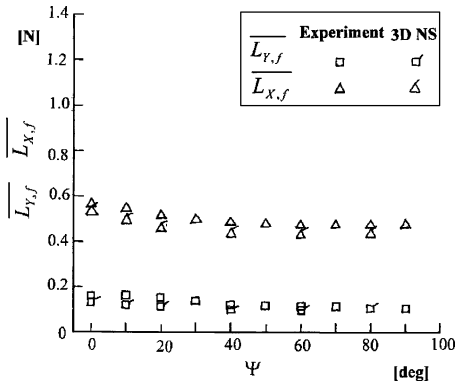

Fig. 10 Variations of forewing time mean forces $\overline{L_{Y,f}}$ and $\overline{L_{X,f}}$ with respect to Ψ.

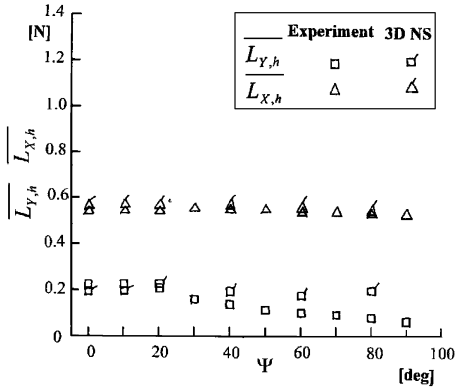

Fig. 11 Variations of hindwing time mean forces $\overline{L_{Y,h}}$ and $\overline{L_{X,h}}$ with respect to Ψ.

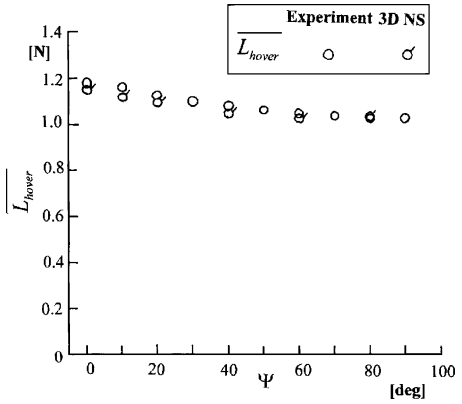

Fig. 12 Variation of $\overline{L_{\text{hover}}}$ with respect to Ψ.

In Figs. 10 and 11, the experimentally determined variations of $\overline{L_Y}$ and $\overline{L_X}$ for the fore- and hindwings with respect to Ψ are presented and compared with those predicted by the NS simulations.

The agreement of these forces between the experiment and the NS simulations is quite good, except that on the hindwing $\overline{L_{Y,h}}$ shows some discrepancy for $\Psi = 60$ and 80 deg. In Figs. 12 and 13, the experimentally measured variations of $\overline{L_{\text{hover}}}$ and ϕ_s with respect to Ψ are compared to the NS predictions. The agreement of $\overline{L_{\text{hover}}}$ is quite good, although there is a discrepancy (about 4–7 deg) in ϕ_s for $\Psi = 60$ and 80 deg. The discrepancy in ϕ_s clearly comes from the discrepancy in $\overline{L_{Y,h}}$ seen in Fig. 11. The reason for this discrepancy has not yet been determined. In Figs. 14, the variations of $\overline{P_f}$, $\overline{P_h}$, and $\overline{P_t}$ with respect to Ψ are plotted and compared with predictions from the NS simulation. The agreement is quite good.

Note that the effects of Ψ, namely, the phase difference between the flapping motions of the fore- and hindwings, on the forces and rate of work are not large, although the magnitudes of the time mean forces and rate of work decrease with an increase in Ψ.

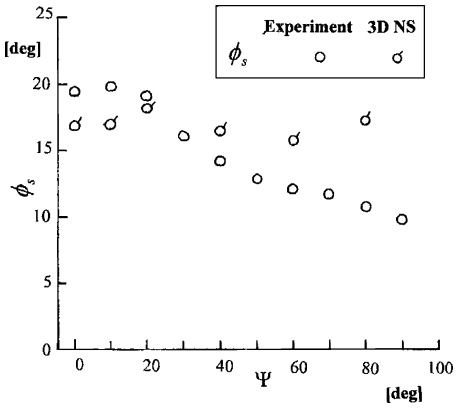

Fig. 13 Variation of ϕ_s with respect to Ψ.

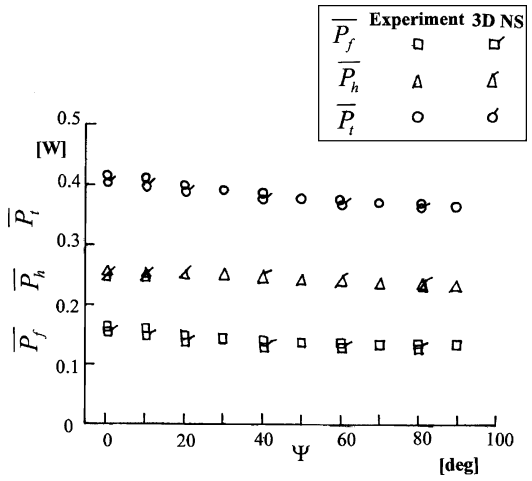

Fig. 14 Variations of $\overline{P_f}$, $\overline{P_h}$, and $\overline{P_t}$ with respect to Ψ.

IV. Conclusions

An experimental study of the dragonfly *Anax parthenope julius* in its hovering mode has been conducted. Measurements are made on a mechanical flapping wing apparatus that dynamically simulates the tandem wing configuration of the dragonfly. This apparatus allows the flow interaction between the fore- and hindwings to be examined; this is accomplished by varying the phase difference between the fore- and hindwings independently of the flapping and feathering motions. The measured time histories of the fluid dynamic forces and the rate of work are compared with the predictions from a previously developed three-dimensional NS code: Overall the agreement between experiment and predicted time histories is good. The phase difference between the flapping motions of the fore- and hindwings is shown to only have a small effect on the time mean values of the forces and the rate of work; this observation indicates that there is only a small degree of flow interaction between the wings when the dragonfly is its hovering mode. The good agreement between three-dimensional NS simulations and experiment suggests that the present NS code may be a useful design tool for insectlike microair vehicles.

Acknowledgments

The authors express their great appreciation to Manabu Matsubara and Masahide Yamasaki of Kyushu University for their kind advice and help in designing and construction of the mechanical flapping apparatus. Without their support, the present experimental study would not have been possible.

References

[1]Weis-Fogh, T., "Quick Estimate of Flight Fitness in Hovering Animals, Including Novel Mechanism for Lift Production," *Journal of Experimental Biology*,Vol. 59, 1973, pp. 169–230.

[2]Norberg, R. A., "Hovering Flight of the Dragonfly Aeshna juncea L.," *Swimming and Flying in Nature*, Vol. 2, Plenum, New York, 1975, pp. 763–781.

[3]Savage, S. B., Newman, B. G., and Wong, D. T. B., "The Role of Vortices and Unsteady Effects During the Hovering Flight of Dragonflies," *Journal of Experimental Biology*, Vol. 83, 1979, pp. 59–77.

[4]Somps, C., and Luttges, M., "Novel Uses of Unsteady Separated Flows," *Science*, Vol. 228, No. 14, 1985, pp. 1326–1329.

[5]Azuma, A., and Watanabe, T., "Flight Performance of a Dragonfly," *Journal of Experimental Biology*, Vol. 137, 1988, pp. 221–252.

[6]Saharon, D., and Luttges, M. W., "Visualization of Unsteady Separated Flow Produced by Mechanically Driven Dragonfly Wing Kinematics Model," AIAA Paper 88-569, 1988.

[7]Freymuth, P., "Thrust Generation by an Airfoil in Hover-Modes," *Experiments in Fluids*, Vol. 9, 1990, pp. 17–24.

[8]Ellington, C. P., van den Berg, C., Willmot, A. P., and Thomas, A. L. R., "Leading Edge Vortices in Insect Flight," *Nature*, Vol. 384, 1996, pp. 626–630.

[9]Wakeling, J. M., and Ellington, C. P., "Dragonfly Flight II. Velocity, Accelerations and Kinematics of Flapping Flight," *Journal of Experimental Biology*, Vol. 200, 1997, pp. 557–582.

[10]Dickinson, M. H., Lehmann, F. O., and Sane, S. P., "Wing Rotation and the Aerodynamic Basis of Insect Flight," *Science*, Vol. 284, June 1999, pp. 1954–1960.

[11]Sunada, S., Kawachi, K., Matsunoto, A., and Sakaguchi, A., "Unsteady Forces on a Two-Dimensional Wing in Plunging and Pitching Motions," *AIAA Journal*, Vol. 39, No. 7, 2001, pp. 1230–1239.

[12]Isogai, K., Fujishiro, S., Saitoh, T., Yamasaki, M., and Matsubara, M., "Study on Aerodynamic Mechanism of Hovering Flight of Dragonfly by Using a Robot," *Proceedings of Second International Symposium on Aqua Bio-Mechanisms* [CD-ROM], Tokai Univ., Kanagawa, Japan, Paper S.3-02, 2003.

[13]Heathcote, S., Martin, D., and Gursul, I., "Flexible Flapping Aifoil Propulsion at Zero Freestream Velocity," *AIAA Journal*, Vol. 42, No.11, 2004, pp. 2196–2204.

[14]Gustafson, K., and Leben, R., "Computation of Dragonfly Aerodynamics," *Computer Physics Communications*, Vol. 65, 1991, pp. 121–132.

[15]Wakeling, J. M., and Ellington, C. P., "Dragonfly Flight III. Lift and Power Requirements," *Journal of Experimental Biology*, Vol. 200, 1997, pp. 583–600.

[16]Isogai, K., and Shinmoto, Y., "Numerical Simulation and Visualization of Unsteady Viscous Flow Around an Oscillating Tandem Airfoil in Hovering Mode," *Proceedings of the 2nd Pacific Symposium on Flow Visualization and Image Processing*, edited by S. Mochizuki, Tokyo Univ. of Agriculture and Technology, Tokyo, 1999.

[17]Wang, Z. J., "Two Dimensional Mechanism for Insect Hovering," *Physical Review Letters*, Vol. 85, No. 10, 2000, pp. 2216–2219.

[18]Saharon, D., and Chakravarthy, S., "Computational and Experimental Studies of Asymmetric Pitch/Plunge Flapping—The Secret of Biological Flyers," AIAA Paper 2001-0859, 2001.

[19]Isogai, K., and Shinmoto, Y., "Study on Aerodynamic Mechanism of Hovering Insects," AIAA Paper 2001-2470, June 2001.

[20]Lan, S. L., and Sun, M., "Aerodynamic Interactions of Two-Airfoils in Unsteady Motion," *Acta Mechanica*, Vol. 150, 2001, pp. 39–51.

[21]Kim, D., and Choi, H., "Vortical Motion Caused by Two Flapping Wings," *Proceedings of Second International Symposium on Aqua Biomechanisms* [CD-ROM], Tokai Univ., Kanagawa, Japan, Paper S.3-05, 2003.

[22]Traub, L. W., "Analysis and Estimation of the Lift Components of Hovering Insects," *Journal of Aircraft*, Vol. 41, No. 2, 2004, pp. 284–289.

[23]Isogai, K., Fujishiro, S., Saitoh, T., Yamashaki, M., and Matsubara, M., "Unsteady Three-Dimensional Viscous Flow Simulation of a Dragonfly Hovering," *AIAA Journal*, Vol. 42, No. 10, 2004, pp. 2053–2058.

N. Chokani
Associate Editor